Prediction of the rotational spectra of microsolvated complexes with low cost DFT methods.

Pablo Pinacho[a], Juan Carlos López[a], Susana Blanco[a]*.

[a] Physical Chemistry Department, University of Valladolid, Paseo Belén 7, 47011 Valladolid, Spain.

* Corresponding author: Susana Blanco, sblanco@qf.uva.es

Abstract

Some of the most used DFT methods together with MP2 have been tested using 6-311++G(d,p) and TZVP basis sets to probe their usefulness in prediction of the rotational spectra of several microsolvated complexes of formamide, *t*-*N*-methylformamide, glycine and β-propiolactone. Results obtained for the rotational parameters and the prediction of the spectra have been compared to experimental data previously measured by Fourier Transform Microwave Spectroscopy. Analysis of the standard deviation of the predicted rotational spectra for all the levels tested indicates that the methods which better approach to the MP2 results are mPW91LYP and B3LYP-D3.

Keywords: Hydrogen Bond, Microwave Spectroscopy, Microsolvation Clusters, Structure, Density Functional Theory.

1. Introduction

The changes in the molecular structure in going to solution environment is a main subject to chemistry since solvation can affect the properties and reactivity of chemical species. Many phenomena associated to solvation can be found in the field of biomolecules. Molecular shape, protein folding [1] or conformational equilibria [2] are only some examples. The evolution of the spectroscopic techniques in combination with supersonic jets, has allowed the isolation of microsolvated molecules with different hydration degrees making possible to understand the role of the solvation forces present in solution at a molecular level. Microwave Spectroscopy has contributed heavily in this field with many studies of microsolvated organic molecules [3]. The inherent flexibility of these complexes, yielding many possible conformers, make the prediction of the rotational spectra a difficult task. Besides, the spectra of the monomers and all possible complexes are present simultaneously, so reasonable good simulations of the spectra are needed in order to assign the different species. *Ab initio* computations are of great help to predict the structures and energies of the possible complexes and their most stable conformers. One of the most used levels of theory is MP2/6-311++G(d,p) which for systems of a reasonable size can be used to have rather good starting predictions of the spectra. This is based on the rotational constants, quadrupole coupling constants and dipole moments obtained from geometry optimization of the different possible conformers. There are methods giving very accurate predictions of the rotational parameters [4] but those are based in a composite scheme of different methods and levels that account for basis sets and correlation effects with a higher computational effort. When the size of the system [5] and the number of water molecules increase [6,7], the calculations with those levels of theory are time-consuming and increase the requirements of the computer properties. An alternative has been using Density Functional Theory (DFT) [8] methods which requires much less computational resources. So that it could be useful to test those methods to see which one gives best overall results for the prediction of

the spectra taking into account the balance between computation cost and the accuracy of the results, which is the aim of this work.

In this context, geometry optimization for several water complexes previously studied by rotational spectroscopy have been done with different DFT methods and compared to MP2 and the experiment. Selected complexes cover several of the most important possible interactions in microsolvation processes. As a reference we have chosen the microsolvation complexes of formamide (FMA) with one and two water molecules. This system serves as a model of interaction between water and peptide bond in proteins. The experimentally observed geometries [9] are depicted in Figure 1.

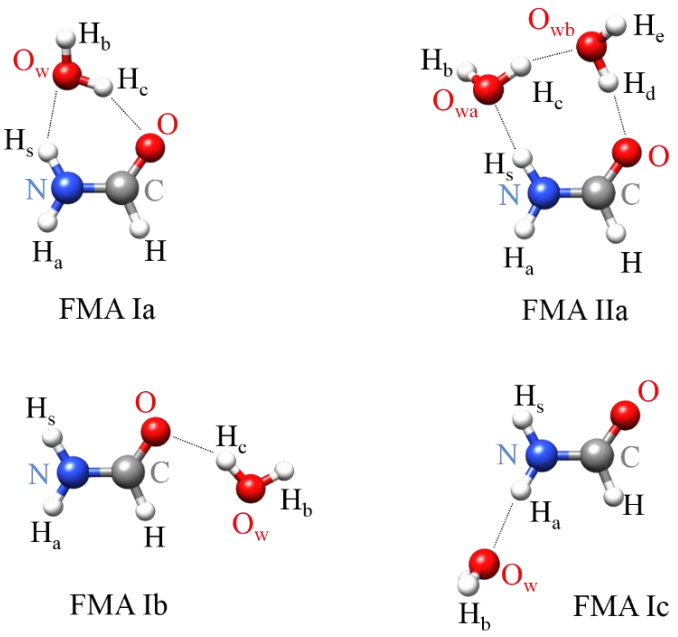

Figure 1. Observed complexes of formamide with one and two molecules of water [9].

Microsolvated complexes of *N*-methylformamide (NMF) are also a good model for the study of interaction between water and the peptide linkage. NMF has *cis* and *trans* conformations, but only *t*-NMF complexes have been observed. The experimentally observed geometries [10] are depicted in Figure 2.

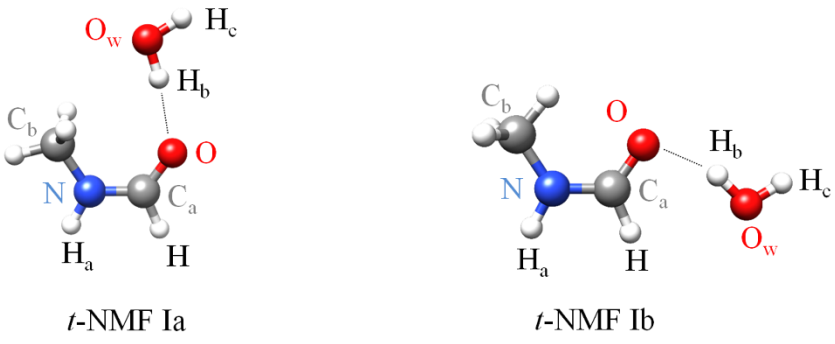

Figure 2. Observed complexes of *t-N*-methyl formamide with one molecule of water [10].

We have also considered the gas phase complexes of glycine (GLY), the simplest amino acid, with one and two molecules of water. In gas phase conditions glycine adopts several conformations, but microsolvated complexes have been observed experimentally only with the lowest energy configuration of glycine [11], as shown in Figure 3.

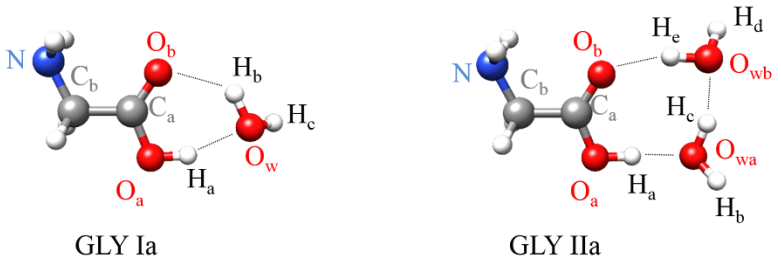

Figure 3. Observed complexes of glycine with one and two molecules of water [11].

β-propiolactone (BPL) is a four-membered plane ring molecule which has been studied microsolvated with up to five water molecules [7] and shows interesting features as n→π* interactions. In this work we have analyzed the results of theoretical calculations for the microsolvated complexes with one and two molecules of water depicted in Figure 4.

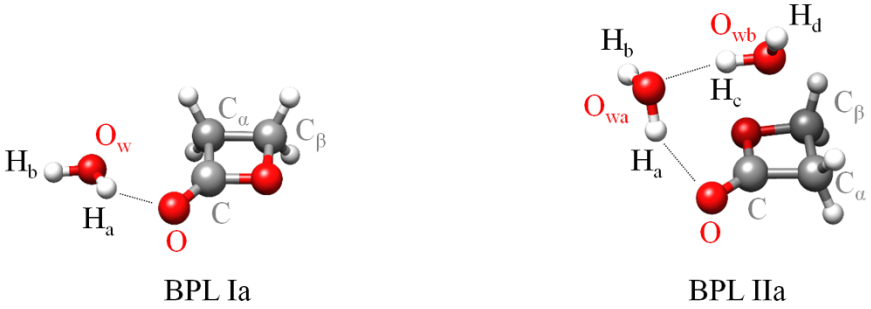

Figure 4. Observed complexes of β-propiolactone with one and two water molecules [7].

2. Computational methods

All the calculations have been done using Gaussian G09 [12]. A total of 13 DFT functionals described below have been used together with MP2 method [13] combined with two basis sets to optimize the geometry of the different molecular complexes. This allows to calculate the different spectroscopic parameters needed to have initial predictions of the rotational spectra. In this case we have to remark that all the calculations correspond to equilibrium geometries while vibrational contributions have not been taken into account.

The unique *ab initio* method used in this work has been MP2. In this method, the Møller-Plesset perturbation theory allows implementing corrections for the electronic correlation in several orders. We have selected second order correction in the frozen core approximation as a reference for several reasons: It gives rather good results in the prediction of the geometry and spectroscopic parameters in a variety of systems including hydrogen bonded ones and for its

affordable computational cost compared to other higher level *ab initio* methods. It is well known that MP2 usually overestimates the barriers involved in large amplitude motions associated to the existence of equivalent conformers but in general it gives reasonable results [14].

DFT is an alternative to obtain the molecular geometry and energy [8]. Many different functionals have been developed accounting for exchange and correlation expressions. From their combination many different DFT methods arise, each one useful to predict different properties of molecular systems. We have evaluated the performance of the functionals: BLYP, B3LYP, B3LYP-D3, X3LYP, mPW91LYP, PBE1PBE, mPW91PBE, PW91PBE, B3PW91, M06, M06-L, M06-2X and TPSSh. DFT functionals performance has been widely studied in biological environment and for organic hydrates [15]. Those used in this work have been selected because they have proved to perform reasonably well for hydrogen bonds, for their popularity in calculations or because they are designed for long-range interactions.

BLYP is a popular functional arising from the combination of Becke's exchange functional [16] together with Lee, Yang and Parr correlation functional [17]. B3LYP is a hybrid functional using 3 experimental parameters fitted by Becke to combine the HF exchange expression along with the Lee-Yang-Parr correlation functional [17,18]. We have included this functional because is the most popular despite it has been reported that has difficulties in predicting accurate structures involving hydrogen bond interactions [19] due to a poor description of dispersion forces. To minimize this problem we included the empirical dispersion correction (GD3) by Grimme (B3LYP-D3) [20]. X3LYP is a hybrid functional developed by Xu to describe non-bonded interactions [17,21].

Perdew, Burke and Ernzerhof´s PBE1PBE, most known as PBE0, is a pure functional converted into a hybrid one [22]. Performance of this functional for hydrogen bonded systems has been widely studied with good results [19,23]. Modified and unmodified PW91 exchange functional [24] combined with Perdew, Burke and Ernzerhof (PBE) gradient corrected correlation functional result in mPW91PBE and PW91PBE. The same mPW91 exchange functional together with Lee, Yang and Parr correlation functional gives rise to mPW91LYP [17,24].

The B3PW91 functional combines the Becke parameters [18] with Perdew and Wang correlation functional [24]. The TPSSh is a hybrid version of Tao, Perdew, Staroverov and Scuseria gradient corrected functional [25].

The hybrid functionals M06 and M06-2X [26] and the pure functional M06-L [27] come from the Minnesota 06 suites of functionals.

Basis set selection is critical to adequately describe the orbitals involved in the hydrogen bonds. In a first step, we tested the basis sets [12]: 6-311++G(d,p), 6-311++G(3df,3dp), cc-pVDZ, aug-cc-pVDZ and TZVP on the complexes of formamide and water combined with PBE0, B3LYP and MP2 methods. The cc-pVDZ basis set does not describe satisfactorily the systems and its results are far from being acceptable. On the contrary, 6-311++G(3df,3dp) guaranties a good description and requires higher computational resources but the results do not constitute a big improvement in comparison with 6-311++G(d,p) basis set. Similar behavior is observed when comparing the results for aug-cc-pVDZ and TZVP basis sets. According to this, we have finally selected Pople´s 6-311++G(d,p) [28], which implements polarization and diffuse functions to improve description of the non-covalent interactions, and Ahlrichs´s triple-ζ TZVP [29], which includes polarization functions. These basis sets are adequate for geometry optimization of the

studied complexes since both describe correctly the atoms of the two first rows of periodic table and are not too big to require excessive computational resources.

3. Results and Discussion

3.1. Conformers of the formamide···$(H_2O)_n$ complexes.

The experimentally observed 1:1 and 1:2 complexes of formamide-water are shown in Figure 1. In the most stable 1:1 complex, Ia, two hydrogen bonds are established. Both molecules act simultaneously as hydrogen donors and acceptors and close a cyclic structure. The calculated hydrogen bond parameters for a representative selection of all the methods with the 6-311++G(d,p) basis set are compared to the experimental r_0 geometry in Table 1. The corresponding rotational constants are compared in Table 2. Tables S1-S4 in supplementary material collect the complete set of the calculated data.

Table 1. Experimental (r_0) and theoretical (r_e) values of the hydrogen bond interaction for conformer Ia of the complex formamide···(H_2O) for a selection of methods using 6-311++G(d,p) basis set.

Parameter[a]	Exp.[b]	BLYP	B3LYP-D3	mPW91LYP	M06-2X	MP2
$r(H_s\cdots O_w)$/ Å	2.061(4)[c]	2.07	2.06	2.05	2.01	2.05
$r(H_c\cdots O)$/ Å	1.93(1)	1.93	1.92	1.92	1.91	1.95
$\angle(N–H_s\cdots O_w)$/ deg	139.5(3)	137.3	137.2	137.0	137.0	138.2
$\angle(H_s\cdots O_w–H_c)$/ deg	78.2(6)	82.2	83.1	83.3	85.4	83.1
$\angle(O_w–H_c\cdots O)$/ deg	153(1)	148.2	147.0	146.9	144.8	146.5
$\angle(H_c\cdots O{=}C)$/ deg	110.3(3)	108.0	108.4	108.4	108.4	107.6
$\tau(H_b–O_w–H_c–H_s)$/ deg	165(1)	139.9	141.0	145.9	152.7	143.0

[a] Atom labeling as in Figure 1. [b] Values reported in reference 9b. [c] Standard error in units of the last digit.

The experimental results [9b] show that the complex is almost planar as indicated by the value of the planar moment P_{cc} (0.054 uÅ^2) which give the mass extension out of the *ab* plane. The calculated values range from 0.149 uÅ^2 for M06-2X/6-311++G(d,p) to 0.481 uÅ^2 for PW91PBE/TZVP (Tables S3-S4). The complex is predicted to have two equivalent conformers with the non-bonded hydrogen atom of water lying out of the *ab* plane at equilibrium with formamide slightly non-planar. Out of plane P_{cc} contributions come mainly from the out of plane hydrogen atom. This is shown from the correlation between the calculated values of P_{cc} and the dihedral angle τ given in Table 1. However, it should be noted that if ground state is above the barrier at the planar configuration, the experimental value would reflect an almost planar structure.

Table 2. Experimental and theoretical values of the rotational parameters for conformer Ia of the complex formamide···(H_2O) for a selection of methods using 6-311++G(d,p) basis set.

	Exp.[e]	BLYP	B3LYP-D3	mPW91LYP	M06-2X	MP2
A[a]/ MHz	11227.9330(23)[f]	10950.5	11154.6	11199.8	11250.8	11067.5
B/ MHz	4586.9623(16)	4587.1	4659.3	4679.2	4774.1	4628.0
C/ MHz	3258.8277(12)	3245.8	3299.0	3310.1	3358.4	3279.4
P_{cc}[b]/ uÅ^2	0.054070(52)	0.311	0.291	0.227	0.149	0.377
χ_{aa}[c]/ MHz	1.3321(37)	1.48	1.50	1.51	1.45	1.37
χ_{bb}/ MHz	2.0371(20)	2.30	2.31	2.31	2.21	2.18
χ_{cc}/ MHz	-3.3693(96)	-3.78	-3.81	-3.82	-3.66	-3.56
σ[d]/ MHz	-	14.4	60.7	77.5	156.8	34.1

[a] A, B, C are the rotational constants. [b] Planar moment $P_{cc} = (I_a + I_b - I_c)/2 = \sum_i m_i c_i^2$. [c] χ_{xy} *(x.y = a, b* or *c)* are the ^{14}N nuclear quadrupole coupling constants. [d] Standard deviation of the prediction considering the R-branch *a*-type transitions. [e] Values reported in reference 9b. [f] Standard error in units of the last digit.

The geometrical parameters other than this dihedral angle could show discrepancies with the experimental data, but since the effective structure is obtained from a fit of the rotational constants, it is perhaps better to directly compare the experimental and theoretical values of the rotational parameters in order to test the methods. This comparison can be seen in Table 2 and in Tables S3-S4 in supplementary material. The *B* rotational constant is systematically predicted to be higher than the experimental value, while *A* and *C* have values lower or higher. The most typical case for large deviations of theory and experiment are shown by the *A* rotational constant. In general, all levels of theory give a value of this constant much worse than of *B* and *C*, introducing a source of error in the prediction of the spectrum. However, in many cases the complexes behave as near-prolate rotors with a μ_a dipole moment component of reasonable magnitude. The R-branch *a*-type spectrum is dominant and strongly dependent on the value of *B*+*C*, being less dependent on the *A* value. Attending to this fact, simple comparison of the values for molecular parameters might not be good enough to discriminate whether a level of theory performs better to predict the spectrum. Instead we have used the standard deviation of the prediction, σ, calculated from the differences between observed and predicted R-branch *a*-type frequencies.

Table 3 and Figures 5 and 6, summarize the values for σ obtained for all the complexes studied in this work. For formamide···(H_2O) Ia it shows slight differences between the two basis sets, been the results of 6-311++G(d,p) basis set better in general. Apart from MP2, the best performance is observed for those DFT methods including LYP correlational functional, being BLYP the method which gives the best agreement. The results obtained with PBE and M06 families are worst because they give a specially deviated value for rotational constant *B*, yielding bad predictions of the spectrum, although rotational constant *A* is reasonably well determined as shown in Tables S3-S4 in supplementary material. The quadrupole coupling constants needed to predict hyperfine structure give in all cases reasonable values.

Table 3. Standard deviation (σ/ MHz) corresponding to the comparison of the observed R-branch *a*-type spectra prediction for all microsolvated complexes considered in this work with those calculated with the different levels of theory. The general trends are shown in Figures 5 and 6.

	FMA[b] Ia	FMA Ib	FMA Ic	FMA IIa	*t*-NMF Ia	*t*-NMF Ib	GLY Ia	GLY IIa	BPL Ia	BPL IIa	Average[c]
BLYP/1[a]	14.4	466.1	173.6	3.9	74.5	245.1	54.5	36.2	271.1	288.6	155.9
BLYP/2	10.7	272.2	102.5	18.9	92.3	188.0	40.0	28.2	190.0	195.3	106.8
B3LYP/1	61.1	251.6	57.7	35.3	36.8	143.1	5.1	11.4	104.6	156.2	87.5
B3LYP/ 2	74.8	141.3	6.6	57.6	36.5	103.1	18.8	13.3	72.5	116.9	68.8
B3LYP-D3/1	60.7	61.1	91.2	57.2	187.7	28.9	11.0	12.3	74.9	107.3	43.7
B3LYP-D3/2	71.3	59.4	135.8	78.0	189.4	33.6	22.9	19.9	80.7	367.7	52.3
X3LYP/1	93.3	113.1	6.7	388.0	54.4	98.6	20.0	11.5	46.1	120.2	110.1
X3LYP/2	108.2	44.6	41.7	73.6	93.3	67.8	34.3	18.0	18.8	81.3	52.2
mPW91LYP/1	77.5	67.6	22.8	39.7	70.3	83.6	12.0	10.1	29.0	121.8	45.6
mPW91LYP/2	94.8	21.3	66.1	63.9	64.8	58.2	27.8	14.8	10.9	71.8	41.7
B3PW91/1	100.5	354.7	50.9	71.6	11.4	192.8	45.6	23.2	180.6	167.5	138.4
B3PW91/2	114.4	211.8	25.6	92.7	10.8	122.4	60.3	30.4	152.1	142.9	112.0
mPW91PBE/1	139.0	182.2	4.6	91.1	25.2	116.8	68.9	34.0	78.2	103.2	101.5
mPW91PBE/2	158.0	92.3	37.2	115.2	25.1	68.3	82.5	42.4	70.6	80.8	89.9
PW91PBE/1	202.6	81.8	4.6	119.3	110.0	79.4	66.4	33.8	53.9	90.5	91.0
PW91PBE/2	215.5	46.2	90.3	145.8	92.7	55.2	81.5	44.0	29.7	38.4	88.3
PBE0/1	156.4	28.6	57.2	97.3	71.2	45.5	74.5	35.6	24.2	74.9	66.0
PBE0/2	180.3	47.6	94.3	123.1	110.5	26.0	89.8	44.7	28.0	54.0	77.1
M06/1	187.2	179.0	483.5	73.4	178.4	80.9	69.2	19.7	126.6	193.5	105.2
M06/2	178.9	153.9	441.1	81.9	175.9	51.8	74.7	21.1	117.4	208.7	97.1
M06-L/1	168.7	12.8	517.0	62.2	177.1	44.8	60.5	15.8	155.5	189.2	74.3
M06-L/2	188.1	71.2	233.7	77.4	164.3	24.3	78.3	22.4	117.9	267.5	82.8
M06-2X/1	156.8	368.6	469.1	65.1	211.3	164.4	49.1	30.3	216.7	386.8	150.1
M06-2X/2	194.9	335.7	383.6	94.5	219.2	171.2	70.3	39.4	233.8	354.5	162.8
TPSSh/1	147.7	77.2	28.6	83.7	37.5	155.9	52.5	22.8	118.0	106.2	94.0
TPSSh/2	160.4	162.6	4.4	105.1	51.8	105.8	64.2	30.0	98.3	74.5	103.8
MP2/1	34.1	11.1	24.6	17.3	101.0	15.2	1.2	1.4	48.1	84.1	18.3
MP2/2	77.0	11.6	72.2	54.2	87.0	16.8	20.9	14.2	37.0	104.7	33.1

[a] 1 refers to 6-311++G(d,p) basis set, 2 refers to TZVP basis set. [b] FMA refers to formamide$\cdots(H_2O)_n$ complexes, *t*-NMF refers to *t*-*N*-methylformamide$\cdots(H_2O)$ complexes, GLY refers to glycine$\cdots(H_2O)_n$ complexes and BPL refers to β-propiolactone$\cdots(H_2O)_n$ complexes. [c] Average of the standard deviation for each method excluding FMA Ic, *t*-NMF Ia and BPL IIa complexes (see conclusions for details).

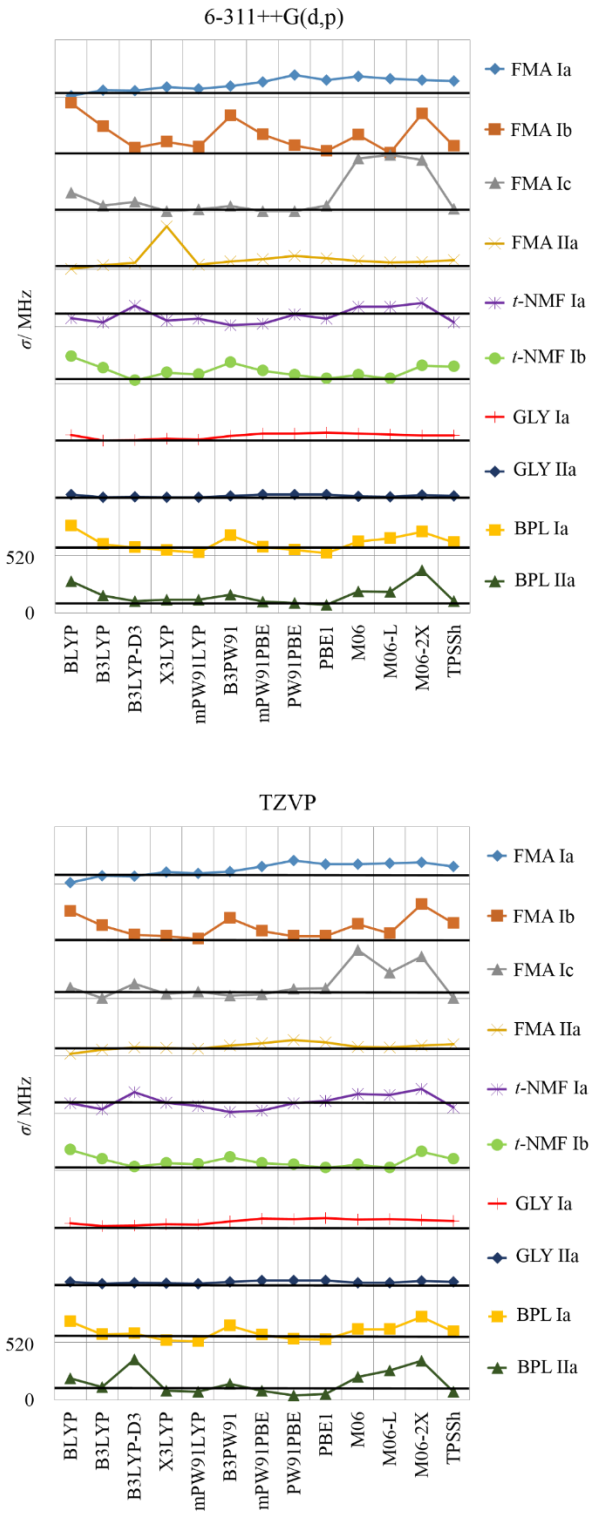

Figure 5. Stacked plot representations showing the variation of the values of the standard deviation (σ/ MHz) collected in Table 3 with the different DFT functionals for each studied complex. The scale for each molecular system is the same showed for BPL IIa (bottom plot). The horizontal straight black lines represent the value of σ obtained for MP2 method taken as a reference. The upper representation corresponds to 6-311++G(d,p) and the lower to TZVP basis sets.

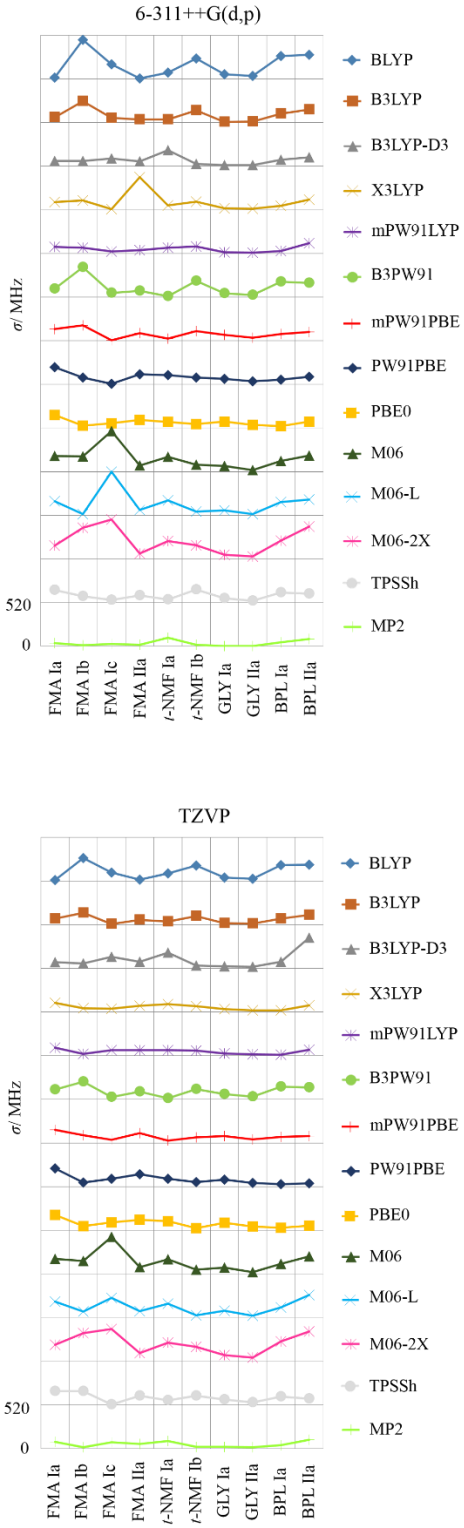

Figure 6. Stacked plot representations showing the variation of the values of the standard deviation (σ/ MHz) collected in Table 3 with the different complex for each studied DFT functionals. The scale for each molecular system is the same showed for MP2 (bottom plot). The upper representation corresponds to 6-311++G(d,p) and the lower to TZVP basis sets.

The IIa conformer (shown in Figure 1) presents three hydrogen bonds closing a sequential cycle between formamide and two molecules of water and could be considered as an extension of formamide···(H_2O) Ia conformer, and in fact, presents a similar behavior. Table 4 presents a selection of results while the whole set of rotational parameters are presented in Tables S7-S8 in supplementary material.

All the atoms except the non-bonded water hydrogens lie in the formamide plane [9b]. These non-bonded hydrogen atoms adopt an up-down configuration. This is reflected in the P_{cc} experimental value of 0.654 uÅ^2. As in conformer Ia the calculations predict a higher value of P_{cc}. This complex presents larger deviation for hydrogen bond parameters when compared to the experimentally derived effective structure even for the levels of theory that better predict the transitions frequencies.

Considering the rotational constants and the value of the standard deviation for the predictions of the spectrum (Table 3 and Figures 5 and 6), there are not big differences between the two basis sets, although in general 6-311++G(d,p) is slightly more accurate than TZVP. BLYP followed by MP2 are the best methods according to the values of σ. The LYP family gives better results, with the exception of X3LYP functional, than M06 and PBE families. As in conformer Ia, the quadrupole coupling constants give reasonable results.

Table 4. Experimental and theoretical values of the rotational parameters for conformer IIa of the complex formamide···(H_2O)$_2$ for a selection of methods using 6-311++G(d,p) basis set.

	Exp.[e]	BLYP	B3LYP-D3	mPW91LYP	M06-2X	MP2
A[a]/ MHz	4384.3559(50)[f]	4364.1	4446.1	4433.2	4458.7	4398.4
B/ MHz	2630.4957(16)	2627.2	2684.8	2665.7	2678.1	2642.6
C/ MHz	1651.1140(13)	1650.3	1685.2	1674.4	1689.3	1661.6
P_{cc}[b]/ uÅ^2	0.65408(24)	0.967	1.004	0.879	1.447	0.993
χ_{aa}[c]/ MHz	1.0739(34)	1.12	1.12	1.17	1.11	1.08
χ_{bb}/ MHz	2.0063(45)	2.32	2.31	2.31	2.15	2.18
χ_{cc}/ MHz	-3.0802(45)	-3.44	-3.44	-3.48	-3.26	-3.25
σ[d]/ MHz	-	3.9	57.2	39.7	65.1	17.3

[a] A, B, C are the rotational constants. [b] Planar moment $P_{cc} = (I_a + I_b - I_c)/2 = \sum_i m_i c_i^2$. [c] χ_{xy} ($x.y = a, b$ or c) are the ^{14}N nuclear quadrupole coupling constants. [d] Standard deviation of the prediction considering the R-branch a-type transitions. [e] Values reported in reference 9b. [f] Standard error in units of the last digit.

In conformer Ib (see Figure 1), the main interaction is the hydrogen bond O-H···O=C stabilized by a weak C-H···O hydrogen bond. This complex shows a small splitting in the rotational spectrum arising from two close vibrational states [9b]. Because the values for rotational parameters are similar in the two states, only the observed values for v=0 have been compared to theoretical constants (Tables S11-S12). Experimentally the complex appears to be planar and this is well predicted in all cases on the basis of the P_{cc} value.

Considering the standard deviation (see Table 3 and Figures 5 and 6), MP2 gives the best results, being the TZVP basis set better than 6-311++G(d,p) in practically all cases. LYP methods give results which are very different to those found in Ia and IIa conformers. BLYP provides bad results in this case. B3LYP presents acceptable values only with the empirical dispersion GD3 correction. X3LYP and mPW91LYP yields rather good values. PBE0 and M06-L functionals behave well with the 6-311++G(d,p) basis set. The main difference between conformer Ib and the previous ones comes from the weak secondary hydrogen bond in conformer Ib, which has significant contributions from dispersive forces. The methods which better describe these forces are expected to give better results as occur when comparing B3LYP and B3LYP-D3 methods.

Conformer Ic of the formamide···(H_2O) complex (see Figure 1) is formed from a different hydrogen bond interaction N-H···O established between the amino group to water oxygen. Water acts in this case only as hydrogen acceptor. The lack of another linkage allows water molecule to rotate along the axis of hydrogen bond. Experimentally, this effect was detected as an appreciable splitting in the spectrum [9b]. The intensity of the transitions was weaker than expected due to the splitting making difficult the observation. From the limited transitions observed, only *B*+*C* was determined without any ambiguity. In addition, the fitting of the spectrum did not provide information enough of the vibrational motion and possible vibration-rotation interactions. For this reason, it is difficult to establish any conclusion from the comparison of the experimental and theoretical values of the data. In any case, the results obtained are collected in Table 3 and Tables S13-S14 in supplementary material.

3.2. Conformers of the *t*-*N*-methylformamide···(H_2O) complexes.

In NMF one of the amino hydrogen atoms of formamide is substituted by a CH_3 group. Thus NMF adopts two possible *cis* and *trans* conformers. Only *t*-NMF complexes with water have been observed (see Figure 2) [10]. The position of the methyl group on the same side of the carbonyl group prevents the formation of N-H···O hydrogen bond as occurs in conformers Ia and IIa of formamide. Nevertheless, the most abundant conformer of *t*-NMF···(H_2O) formed by a O-H···O=C bond and weak secondary C-H···O interactions involving the methyl group is labeled Ia for analogy. The second conformer labeled Ib presents the same interactions as conformer Ib of formamide. The results of the calculations are given in Table 3 and Tables S15-S18 in supplementary material.

The weak secondary interaction established between the methyl group and water in conformer Ia is the key factor to define the final conformation predicted by the different methods. A bifurcated interaction with two C-H···O weak hydrogen bonds is predicted but the degree of symmetry of this interaction varies with the method. In some cases, it is almost symmetrical while in other cases one of the two interactions is dominant. This corresponds to different equilibrium arrangements of the CH_3 group which affects to the position of the water molecule with respect to the symmetry plane of NMF. Thus there is an evident interaction with the internal rotation of the methyl group. The predictions of the P_{cc} planar moment reflect this behavior. The experimental value of P_{cc} is 1.876 uÅ^2 while the predictions oscillate around this value which range from 1.56 uÅ^2 for B3LYP-D3 to 3.4 uÅ^2 for MP2/6-311++G(d,p). Considering the standard deviation of the prediction of the spectra (Table 3 and Figures 5 and 6), the LYP family seems to work well with the exception of B3LYP-D3. B3PW91 seems to be optimal with any of the two basis sets as well as mPW91PBE and TPSSh. MP2 and B3LYP-D3, which work fine in other cases, do not give good results here.

Conformer Ib is expected to have a low V_3 barrier similar to that of bare *t*-NMF and this affects to the effective values of the rotational constants as pointed out by Caminati *et al*. [10]. As an example, we can cite the effective value of P_{cc} = 0.793 uÅ^2 which, corrected from the contributions of the methyl group internal rotation, is estimated to be 1.59 uÅ^2. This value is closer to the theoretical values than the effective one and corresponds to an essentially planar skeleton with two out of plane hydrogen atoms, as predicted. Taking into account this fact, some corrections should be made in the predicted rotational constants if internal rotation data were *a priori* known, not being the case. In any case, the behavior of the different methods with respect to standard deviation seem to be correlated with that observed for conformer Ib of formamide water complex, although the result seems to be apparently better (see Tables 3, S17-S18 and Figures 5 and 6). This can be associated to the fact that hydrogen bond interactions are the same in both complexes.

3.3. Conformers of the glycine$\cdots(H_2O)_n$ complexes.

The complexes of glycine with water are very important systems since they had provided the first model for the interactions of amino acids with water [11]. In glycine$\cdots(H_2O)$ and glycine$\cdots(H_2O)_2$ both the water molecules and the carboxyl group act simultaneously as hydrogen donors or acceptors. By this reason, glycine carboxyl group and water molecules close sequential cycles similar to those found for formamide water complexes as shown in Figure 3. The configuration of the non-bonded hydrogen atoms of water molecules in glycine$\cdots(H_2O)_2$ is also up-down in this case. For these reasons, we have labeled the observed complexes of glycine$\cdots(H_2O)$ as Ia and glycine$\cdots(H_2O)_2$ as IIa by analogy with formamide water complexes. The results are collected in Table 3 and in Tables S21-S24 in supplementary material.

Both complexes have a planar skeleton as reflected by the value of P_{cc} which has out of plane contributions from the hydrogen atoms of methylene and amino groups as well as from the non-bonded water hydrogen atoms. The experimental values of P_{cc} = 3.199 uÅ^2 for conformer Ia and P_{cc} = 3.699 uÅ^2 for conformer IIa are reasonable well reproduced taking into account that the experimental value corresponds to a ground vibrational state average and the predictions to equilibrium conformers. The same can be seen for the structural parameters of the hydrogen bond in glycine$\cdots(H_2O)$ as shown in Tables S19-S20 in supplementary material.

Considering the prediction of the spectra (see Table 3 and Figures 5 and 6), the best results in this case are obtained for MP2/6-311++G(d,p). All functionals work reasonably well, being the LYP family that showing the best performances. There are not big differences between B3LYP and B3LYP-D3 indicating that electrostatic forces dominate the interactions.

3.4. Conformers of the β-propiolactone$\cdots(H_2O)_n$ complexes.

As we have already mentioned, the microsolvation of BPL has been experimentally studied for complexes up to five water molecules [7]. For the purpose of this work which compares systems with one and two water molecules we have considered only the complexes labeled Ia and IIa for BPL in Figure 4.

In complex Ia, water interacts through an hydrogen bond with the oxygen in the carbonyl group and a weak secondary bifurcated C_α-H$\cdots O_w$ hydrogen bond with the methylene group in α position. The skeleton of the complex presents a planar configuration. The planar moment P_{cc} = 3.470 uÅ^2 collects the contributions of the methylene groups hydrogen atoms and compared to the value of bare BPL (P_{cc} = 3.242 uÅ^2) [7] shows contributions from the non-bonded hydrogen

atom of water molecule or out of plane intermolecular vibrational effects. All DFT functionals predict water molecule being in the symmetry plane of BPL while MP2 locates the non-bonded hydrogen atom of water out of this plane as seen in P_{cc} values collected in Tables S25-S26 in supplementary material. Considering the prediction of the spectrum, TZVP basis set gives better results than 6-311++G(d,p). The best results are obtained with mPW91LYP functional while X3LYP, PW91PBE and PBE0 give also reasonable values of the standard deviation (see Table 3 and Figures 5 and 6).

In complex IIa, the two water molecules close a sequential cycle with BPL through O_{wa}-$H_a\cdots O{=}C$, O_{wb}-$H_c\cdots O_{wa}$ and simultaneous weak C_α-$H\cdots O_{wb}$ and C_β-$H\cdots O_{wb}$ hydrogen bonds. A $n\rightarrow\pi^*$ interaction from the one non-bonded electron pair of O_{wb} to the non-bonding π^* orbital of the carbonyl group may also contribute to stabilize this complex. The two water molecules lie out of the ring plane in a *quasi*-perpendicular arrangement which is reflected by the P_{cc} value of 51.077 u$Å^2$ which is well predicted by M06 and MP2 methods (see Tables S27-S28). In general, the prediction of the spectrum (see Table 3 and Figures 5 and 6) is not very good except for the PW91PBE/TZVP. Probably the description of the weak interactions of H_2O_{wb} with BPL and the possible contribution of intermolecular vibrations are the cause of the deviations. Chemical computations have difficulties in determine precisely the position of the water molecules and there are variations with the level of theory. Even small differences in the disposition of the oxygen atom led to big differences in the rotational constants and large deviations in the prediction of the spectrum.

4. Conclusions

In order to establish some conclusions, we can analyze the results summarized in Table 3 for the standard deviation of the predictions of the R-branch *a*-type spectra, as we have explained in previous sections. Figures 5 and 6, which represent the values given in Table 3, show a noticeable dispersion of the values of σ arising by the different nature of the intermolecular interactions in each system, the presence of large amplitude intramolecular vibrations and the different kind of functionals used. Despite this apparent dispersion, it is possible to find some interesting correlations between systems with similar interactions as shown in Figure 7.

In these plots we represent the values of σ obtained with the same method of different systems *vs* those of formamide water complexes which represent all possible kind of interactions. For example formamide$\cdots(H_2O)$ Ia is formed by two moderate hydrogen bonds as occurs for glycine$\cdots(H_2O)$ Ia (see Figures 1 and 3). Figure 7a shows the linear correlation existing between the results of both systems for the different calculations. Formamide$\cdots(H_2O)_2$ IIa and glycine$\cdots(H_2O)_2$ IIa can be compared in the same way as is shown in Figure 7b. Formamide$\cdots(H_2O)$ Ib presents a moderate O-H$\cdots$O=C hydrogen bond and a weak C-H$\cdots$O interaction. Similar configurations occur for *t*-NMF$\cdots(H_2O)$ Ib and BPL$\cdots(H_2O)$ Ia and in fact a linear correlation exists between the results for these systems as can be seen in Figure 7c. An interesting feature can be also observed in Figure 7 concerning the dispersion of the values and the relative stability of the complexes. The highest dispersion corresponds to formamide$\cdots(H_2O)$ Ib type interactions which are the less stable systems [9b]. Formamide$\cdots(H_2O)$ Ia interactions correspond to the most stable 1:1 complexes and show a noticeable smaller dispersion compared to Ib type conformers. This trend is more pronounced in the 1:2 complexes which are further stabilized by hydrogen bond cooperativity [30].

The rest of systems cannot be considered within those correlations since they present different interactions. For example, formamide···(H_2O) Ic has only one hydrogen bond and shows an almost free rotation of the water molecule. *t*-NMF···(H_2O) Ia is affected by the internal rotation of the methyl group interacting with water. In BPL···(H_2O)$_2$ IIa one of water molecules interacts with BPL molecule through a hydrogen bond and the other through weak secondary n→π* interactions.

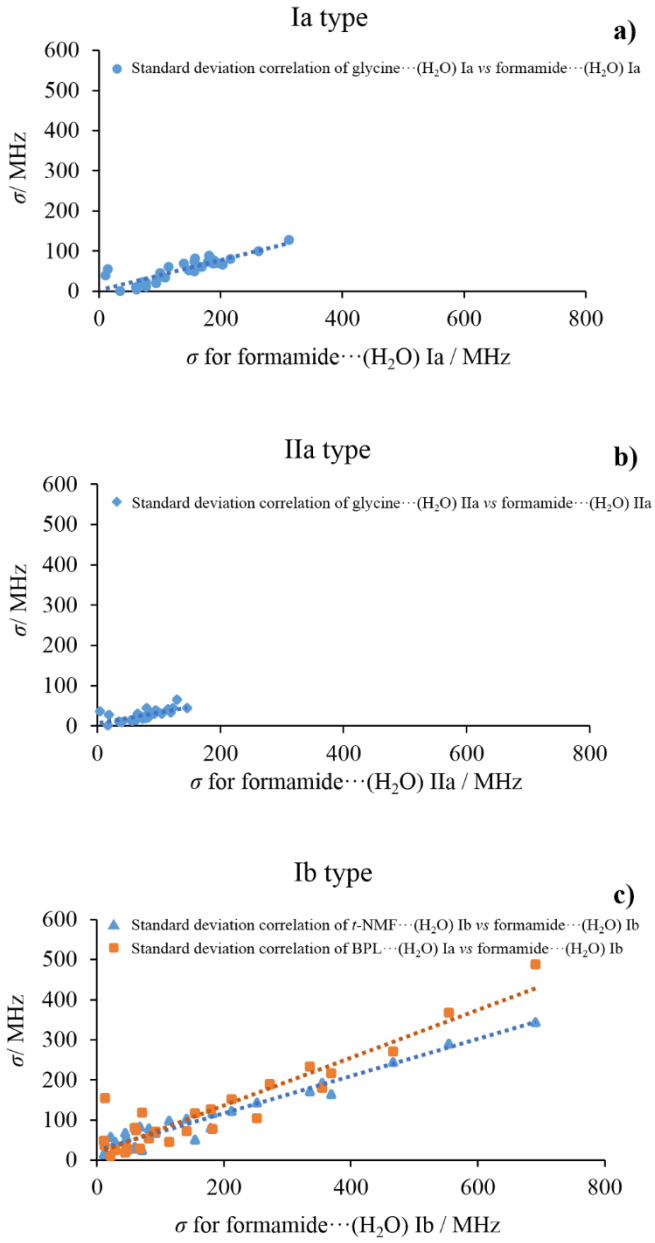

Figure 7. Standard deviation correlations of a) glycine···(H_2O) Ia *vs* formamide···(H_2O) Ia. b) glycine···(H_2O)$_2$ IIa *vs* formamide···(H_2O)$_2$ IIa. c) *t*-NMF···(H_2O) Ib (blue triangles) and BPL···(H_2O) Ia (orange squares) *vs* formamide···(H_2O) Ib.

Not all levels of theory perform equally. Considering the average results for σ (see Table 3), the best performance is, as could be expected, that of MP2 with both basis sets. For the DFT functionals the best results corresponds to mPW91LYP and B3LYP-D3 being the dispersion of the values narrower for B3LYP-D3. This behavior is clearly reflected in Figures 5 and 6. The use of these methods could be suggested in large systems as an alternative to MP2 since they have a lower computational cost.

Funding: This work was supported by the Junta de Castilla y León (UNVA-13-3E-2103).

Acknowledgments: SB and JCL would like to express their deep gratitude to Professor W. Caminati. We have learned so much from him while cooperating in many interesting problems. We also have had the privilege of enjoying his friendship, hospitality and kindness everywhere.

5. References

[1] a) D. Liu, T. Wyttenbach, C. J. Carpenter, M. T. Bowers, J. Am. Chem. Soc. 126 (2004) 3261-3270. b) A. R. Bizzarri, S. Cannistraro, J. Phys. Chem. B 106 (2002) 6617-6633. c) W. Blokzijl, J. B. F. N. Engberts, Angew. Chem. Int. Ed. 32 (1993) 1545-1579.
[2] M. Schmitt, M. Böhm, C. Ratzer, C. Vu, I. Kalkman, W. L. Meerts, J. Am. Chem. Soc. 127 (2005) 10356-10364.
[3] W. Caminati, J. U. Grabow, in: J. Laane (ed.), Frontiers of Molecular Spectroscopy, Elsevier, Amsterdam, 2009, pp. 383-454.
[4] a) C. Puzzarini, Int. J. Quantum Chem. 116 (2016) 1513-1519. b) C. Puzzarini, V. Barone, Phys. Chem. Chem. Phys. 13 (2011) 7158-7166.
[5] C. Pérez, J. C López, S. Blanco, M. Schnell, J. Phys. Chem. Lett. 7 (2016) 4053-4058.
[6] C. Pérez, A. Krin, A. L. Steber, J. C. López, Z. Kisiel, M. Schnell, J. Phys. Chem. Lett. 7 (2016) 154-160.
[7] C. Pérez, J. L. Neill, M. T. Muckle, D. P. Zaleski, I. Peña, J. C. López, J. L. Alonso, B. H. Pate, Angew. Chem. Int. Ed. 54 (2015) 979–982.
[8] a) P. Hohenberg, W. Kohn, Phys. Rev. 136 (1964) B864-B871. b) W. Kohn, L. J. Sham, Phys. Rev. 140 (1965) A1133-A1138.
[9] a) F. J. Lovas, R. D. Suenram, G. T. Fraser, C. W. Gillies, J. Zozom, J. Chem. Phys. 88 (1988) 722. b) S. Blanco, J. C. López, A. Lesarri, J. L. Alonso, J. Am. Chem. Soc. 128 (2006) 12111-12121. c) S. Blanco, P. Pinacho, J. C. López, Angew. Chem. Int. Ed. 55 (2016) 9331-9335.
[10] W. Caminati, J. C. López, S. Blanco, S. Mata, J. L. Alonso, Phys. Chem. Chem. Phys. 12 (2010) 10230–10234.
[11] a) J. L. Alonso, E. J. Cocinero, A. Lesarri, M. E. Sanz, J. C. López, Angew. Chem. Int. Ed. 45 (2006) 3471-3474. b) J. L. Alonso, I. Peña, M. E. Sanz, V. Vaquero, S. Mata, C. Cabezas, J. C. López, Chem. Commun. 49 (2013) 3443-3445.
[12] Gaussian 09, Revision D.01, M. J. Frisch, G. W. Trucks, H. B. Schlegel, G. E. Scuseria, M. A. Robb, J. R. Cheeseman, G. Scalmani, V. Barone, B. Mennucci, G. A. Petersson, H. Nakatsuji, M. Caricato, X. Li, H. P. Hratchian, A. F. Izmaylov, J. Bloino, G. Zheng, J. L. Sonnenberg, M. Hada, M. Ehara, K. Toyota, R. Fukuda, J. Hasegawa, M. Ishida, T. Nakajima, Y. Honda, O. Kitao, H. Nakai, T. Vreven, J. A. Montgomery, Jr., J. E. Peralta, F. Ogliaro, M. Bearpark, J. J. Heyd, E. Brothers, K. N. Kudin, V. N. Staroverov, R. Kobayashi, J. Normand, K. Raghavachari, A. Rendell, J. C. Burant, S. S. Iyengar, J. Tomasi, M. Cossi, N. Rega, J. M. Millam, M. Klene, J. E. Knox, J. B. Cross, V. Bakken, C. Adamo, J. Jaramillo, R. Gomperts, R. E. Stratmann, O. Yazyev, A. J. Austin, R. Cammi, C. Pomelli, J. W. Ochterski, R. L. Martin, K. Morokuma, V. G. Zakrzewski, G. A. Voth, P. Salvador, J. J. Dannenberg, S. Dapprich, A. D. Daniels, Ö. Farkas, J. B. Foresman, J. V. Ortiz, J. Cioslowski, and D. J. Fox, Gaussian, Inc., Wallingford CT, 2009.
[13] C. Møller, M. S. Plesset, Phys. Rev. 46 (1934) 618-622.
[14] J. C. López et al., Submitted to J. Mol. Spec. (Volume dedicated to Professor W. Caminati).
[15] a) T. Wijst, C. F. Guerra, M. Swart, F. M. Bickelhaupt, Chem. Phys. Lett. 426 (2006) 415-421. b) Y. Liu, J. Zhao, F. Li, Z. Chen, J. Comp. Chem. 34 (2013) 121-131.
[16] A. D. Becke, Phys. Rev. A 38 (1988) 3098-3100.

[17] C. Lee, W. Yang, R.G. Parr, Phys. Rev. B 37 (1988) 785-789.
[18] a) A. D. Becke, J. Chem. Phys. 98 (1993) 5648-5652. b) S. H. Vosko, L. Wilk, M. Nusair, Can. J. Phys. 58 (1980) 1200-1211.
[19] a) Y. Zhao, D. G. Trulhar, J. Chem. Theory Compu. 3 (2007) 289-300. b) Y. Zhao, D. G. Trulhar, J. Chem. Theory Compu. 1 (2005) 415-432.
[20] S. Grimme, J. Antony, S. Ehrlich, H. Krieg, J. Chem. Phys. 132 (2010) 154104:1-19.
[21] X. Xu, W. A. Goddard III, Proc. Natl. Acad. Sci. USA 101 (2004) 2673-2677.
[22] a) J. P. Perdew, K. Burke, M. Ernzerhof, Phys. Rev. Lett. 77 (1996) 3865-3868. b) C. Adamo, V. Barone, J. Chem. Phys. 110 (1999) 6158-6169.
[23] a) S. M. Bachrach, J. Phys. Chem. A 112 (2008) 3722-3730. b) J. Ireta, J. Neugebauer, M. Scheffler, J. Phys. Chem. A 108 (2004) 5692-5698.
[24] J. P. Perdew, P. Ziesche, H. Eschrig, Electronic Structure of Solids ´91, Akademie Verlag, Berlin, 1991.
[25] J. M. Tao, J. P. Perdew, V. N. Staroverov, G. E. Scuseria, Phys. Rev. Lett. 91 (2003) 146401:1-4.
[26] Y. Zhao, D. G. Truhlar, Theor. Chem. Acc. 120 (2008) 215-241.
[27] Y. Zhao, D. G. Truhlar, J. Chem. Phys. 125 (2006) 194101: 1-18.
[28] R. Ditchfield, W. J. Hehre, J. A. Pople, J. Chem. Phys. 54 (1971) 724-728.
[29] A. Schaefer, C. Huber, R. Ahlrichs, J. Chem. Phys. 100 (1994) 5829-5835.
[30] a) G. A. Jeffrey, W. Saenger, Hydrogen Bonding in Biological Structures, Springer-Verlag, New York, 1991. b) G. A. Jeffrey, Introduction to Hydrogen Bonding, Oxford University press, Oxford, 1997.